Phosphine Complexes of Platinum(II) Cycloplatinated Ferrocenylamines

Noel W. Duffy, C. John McAdam, Brian H. Robinson,* and Jim Simpson*

Department of Chemistry, University of Otago, P.O. Box 56, Dunedin, New Zealand

Received February 23, 1994[⊗]

Platinocycles *R,S*-{Pt[(η^5-C_5H_5)Fe(σ,η^5-$C_5H_3CH_2NMe_2$)](η^2-P-P)}$^+$ X^- (P-P = dppm, dppe, dppb, dppf; X = Cl, ClO_4, CF_3SO_3), *R,S*-{Pt[(η^5-C_5H_5)Fe(σ,η^5-$C_5H_3CH_2NMe_2$)]Cl}$_2$(μ^2-P-P) (P-P = dppb, dppbz), and *R,S*-{Pt[(η^5-C_5H_5)Fe(σ,η^5-$C_5H_3CH_2NMe_2$)]Cl(η^1-P-P)} (P-P = dppb, dppbz), with potential cytotoxic properties, have been synthesized by reaction of the ligand with *R,S*-Pt[(η^5-C_5H_5)Fe(σ,η^5-$C_5H_3CH_2NMe_2$)](dmso)Cl and characterized by analytical, conductance, and spectroscopic data. Geometrical isomers of *R,S*-{Pt[(η^5-C_5H_5)Fe(σ,η^5-$C_5H_3CH_2NMe_2$)][η^2-(η^5-$C_5H_4PPh_2$)Fe(η^5-$C_5H_3PPh_2(CH_2NMe_2)$]}$^+$ and *R,S*-{Pt[(η^5-C_5H_5)Fe(σ,η^5-$C_5H_3CH_2NMe_2$)][η^1-(η^5-$C_5H_4PPh_2$)Fe(η^5-$C_5H_3PPh_2(CH_2NMe_2)$]Cl} with a pendant PPh_2 and/or CH_2NMe_2 group are also described. Enantiomeric, diplatinum analogues, *meso*- and *dl*-{Pt_2[(σ,η^5-$C_5H_3CH_2NMe_2$)$_2$Fe](η^2-P-P)$_2$}$^{2+}$ X^-_2 (P-P = dppm, dppe, dppf; X = Cl, CF_3SO_3) were similarly prepared from *meso*- or *dl*-Pt_2[Fe(σ,η^5-$C_5H_3CH_2NMe_2$)$_2$](dmso)$_2Cl_2$ (the latter stereoisomers were separated by a new procedure). X-ray structures of the triflate salts of *S*-{Pt[(η^5-C_5H_5)Fe(σ,η^5-$C_5H_3CH_2NMe_2$)](η^2-dppm)}$^+$ (orthorhombic, $P2_12_12_1$, a = 12.755(2)Å, b = 16.011(3)Å, c = 18.710(3)Å, Z = 4) and *meso*-{Pt_2[(σ,η^5-$C_5H_3CH_2NMe_2$)$_2$Fe](η^2-dppm)$_2$}$^{2+}$ (monoclinic $P2_1/n$, a = 12.335(1)Å, b = 16.102(1)Å, c = 18.856(1)Å; β = 98.82(7)°, Z = 2) delineate the Pt(II) coordination spheres and show that the dppm chelate ring is strained. Structural and spectroscopic data show that coordination of the chelate ligand does not increase intramolecular contacts. Trends in the ^{31}P and ^{195}Pt NMR parameters correlate with chelate ring size.

Platinum(II) compounds with cytotoxic activity include tertiary phosphine derivatives[1,2] as well as the archetypal derivatives, PtN_2Cl_2 (N = amine).[3] With the discovery[4,5] of a new class of cycloplatinated Pt(II)−ferrocenylamine complexes, *R,S*-Pt[(η^5-C_5H_5)Fe(σ,η^5-$C_5H_3CH_2NMe_2$)](dmso)X and *meso*/*dl*-Pt_2[Fe(σ,η^5-$C_5H_3CH_2NMe_2$)$_2$](dmso)$_2X_2$ (X = Cl, Br, I), there was the opportunity to synthesize a series of complexes with potential antiproliferative activity which feature both amine and phosphine functionality. The S-bound dmso ligand trans to the NMe_2 group in the cycloplatinated complexes can be replaced by other π-acceptor ligands, but the σ-PtC bond is not cleaved by either σ-donor or π-acceptor ligands. Given the strong *trans* effect of the σ-bound ferrocenyl group, it was anticipated that the halide group trans to the Pt−(σ-ferrocenylamine) bond would also be labile, providing another coordination position for a bidentate π-acceptor ligand in the Pt(II) coordination sphere. Pt(II) complexes with η^2-P-P coordinated bis(diphenylphosphino)ferrocene[6] or bis(phosphino)ferrocenylamines,[7] {(η^5-C_5H_5)-Fe[η^5-$C_5H_3CH(R')NMe_2(PPh_2)$)}, are well characterized, but in this paper, we describe the synthesis and structure of the first complexes in which chelating phosphines are associated with a cycloplatinated ferrocenylamine ligand and the first examples of an ionic platinocycle with an ferrocenylamine ligand. The ligands were chosen to include those that normally chelate (dppm),[8] those which could chelate or bridge two Pt(II) coordination spheres (dppb, dppe, dppf), those which might provide a rigid link between the cycloplatinated moieties (dppbz), and those where alternative NMe_2 and η^2-P-P functionalities are provided (bppfa). For biological testing, it is important to establish the stereochemistry of the chelated derivatives and therefore procedures have been developed for the convenient separation of the *meso*- and *dl*-Pt_2[Fe(σ,η^5-$C_5H_3CH_2NMe_2$)$_2$](dmso)$_2Cl_2$ stereoisomers.

Experimental Section

Complexes **1** and **2** were prepared from the appropriate ferrocenylamine and $Pt(dmso)_2Cl_2$ as described previously.[4,5] The ligands[8] dppm and dppe were purchased from Strem and dppf,[9] dppb,[10] dppbz,[11] and bppfa[12] prepared by literature methods. Solvents were dried by standard methods and stored under nitrogen. NMR, IR and UV/vis spectra were recorded on a Varian 300 MHz VXR or 200 MHz Gemini, Digilab FTIR, and Perkin Elmer Lambda 9 spectrometers, respectively. NMR were referenced to ^1H (TMS), ^{13}C (TMS), and ^{195}Pt (Na_2PtCl_6). Conductivities were measured in a two-electrode cell standardized with Me_4NCl in acetone. All reactions were carried out in an inert atmosphere, and in the case of the diplatinum(II) derivatives workup was also under nitrogen due to the rapid reaction of these complexes with oxygen; this applies particularly to the *meso*-stereoisomers. Typical preparations and only significant spectral data are given below. Compilations are given in Table 5 and supplementary material (Table S8). All compounds gave satisfactory analyses (performed by the Campbell Microanalytical Laboratory, University of Otago).

⊗ Abstract published in *Advance ACS Abstracts,* October 1, 1994.

(1) Berners-Price, J.; Sadler, P. J. *Struct. Bonding (Berlin)* **1988**, *70*, 27.
(2) Scarcia, V.; Furlani, A.; Longato, B.; Corain, B.; Pilloni, G. *Inorg. Chim. Acta* **1988**, *153*, 67.
(3) Abrams, M. In *The chemistry of antitumour agents*; Wilman, D. E. V., Ed.; Chapman and Hall: London, 1990; p 331. *Platinum and Other Metal Coordination Compounds in Cancer Chemotherapy*; Howell, S. B., Ed.; Plenum Press, New York, 1991.
(4) Ranatunge-Bandarage, P. R. R.; Robinson, B. H.; Simpson. J, *Organometallics* **1994**, *13*, 500.
(5) Ranatunge-Bandarage, P. R. R.; Duffy, N. W.; Johnson, S. M.; Robinson, B. H.; Simpson, J. *Organometallics* **1994**, *13*, 511.
(6) Clemente, D. A.; Pilloni, G.; Corain, B.; Longato, B.; Tiripicchio-Ca-Mellini, M. *Inorg. Chim. Acta* **1986**, *115*, L9.
(7) Heddon, D.; Roundhill, D. M.; Futtz, W. C.; Rheingold, A. C. *Organometallics*, **1986**, *5*, 336.
(8) Dppm ≡ bis(diphenylphosphino)methane. dppe ≡ bis(diphenylphosphino)ethane. dppf ≡ bis(diphenylphosphino)ferrocene. dppb ≡ bis-(*p*-diphenylphosphino)butane. dppbz ≡ bis(*p*-diphenylphosphino)-benzene. bppfa = ((dimethylamino)methyl)bis(diphenylphosphino)-ferrocene.
(9) Bishop, J. J.; Davison, A.; Kotscher, M. L. Ligtenberg, D. W.; Merril, R. E. Smart, J. C. *J. Organomet. Chem.* **1971**, *27*, 241.
(10) Scwarzenbach, A.; Pinkerton, A.; Chapius, G.; Wenger, J.; Ros, R.; Poulet, R. *Inorg. Chim. Acta* **1977**, *25*, 255.
(11) Baldwin, R. A., Cheng, M. T. *J. Org. Chem.*, **1967**, *32*, 1572.
(12) Hayashi, T.; Mise, T.; Fukushima, M.; Kagotani, M.; Nagshima, N.; Hamada, Y.; Matsumoto, A.; Kawakami, S.; Konishi, M.; Yamamoto, K.; Kumada, M. *J. Bull. Chem. Soc. Jpn.* **1980**, *53*, 1138.

0020-1669/94/1333-5343$04.50/0

***R,S*-{Pt[(η^5-C_5H_5)Fe(σ,η^5-$C_5H_3CH_2NMe_2$)]η^2-dppm}$^+X^-$ (3).** *R,S*-**1** (100 mg, 1.82×10^{-4} mol) and dppm (70 mg, 1.82×10^{-4} mol) were added simultaneously to chloroform (25 cm^3). The solution darkened immediately, and the mixture was stirred at 15 °C for 15 min under nitrogen and the solvent then evaporated *in vacuo* to give a red oil; yield of impure **3a** (X = Cl) 202 mg. ^{31}P NMR ($CDCl_3$): −22.0, −32.2. ^{195}Pt NMR ($CDCl_3$, 25 °C): −3970. The other salts were prepared from **3a** by metathetical reactions. A saturated solution of $LiClO_4 \cdot H_2O$ in methanol was added dropwise to **3a** (202 mg) in methanol (1 cm^3) until a yellow precipitate forms. The precipitate was recrystallized from hot methanol to yield brick red crystals of **3c** (X = ClO_4); yield 80%. Similarly **3b** (X = CF_3SO_3) was isolated from **3a** using sodium triflate. Anal. Calcd for $C_{39}H_{38}F_3FeNO_3P_2PtS$: C, 48.26; H, 3.95; N, 1.44. Found: C, 48.11; H, 3.46; N, 1.60. ^{1}H NMR ($CDCl_3$): 2.85 (s, 3H, C*H*$_3$N); 3.23 (s, 3H, C*H*$_3$N); 3.65 (m, 2H, C*H*$_2$N). Conductivity (Λ_m, acetone): 60 Ω^{-1} mol^{-1} dm^2.

***R,S*-{Pt[(η^5-C_5H_5)Fe(σ,η^5-$C_5H_3CH_2NMe_2$)]η^2-dppe}$^+X^-$ (4).** *R,S*-**1** (25 mg, 4.5×10^{-5} mol) was dissolved in chloroform (5 cm^3); upon the addition of dppe (16 mg, 4.4×10^{-5} mol) the solution instantaneously turned red. After 10 min stirring, the solvent was removed *in vacuo* and the residue recrystallized from CH_2Cl_2/ether giving a yellow powder of **4a** (X = Cl); yield 77%. Mp: 212−214 °C. Treatment of **4a** with sodium triflate gave **4b** (X = CF_3SO_3). Anal. Calcd for $C_{39}H_{40}F_3FeNO_3P_2PtS$: C, 53.78; H, 4.63; N, 1.61. Found: C, 52.82; H, 4.81; N, 1.81. ^{1}H NMR ($CDCl_3$): 2.59 (m, 3H, J^1(Pt−H) = 24 Hz, NC*H*$_3$); 2.90 (m, 3H, NC*H*$_3$); 3.43, 3.50, 3.56, 3.70 (C*H*$_2$N and P(C*H*$_2$)$_2$P). Conductivity (Λ_m acetone): 123 Ω^{-1} mol^{-1} dm^2.

Dppb Complexes from 1. *R,S*-**1** (65 mg, 1.18×10^{-4} mol) was dissolved in chloroform (75 cm^3); slow addition of dppb (50 mg, 1.17×10^{-4} mol) in chloroform (25 cm^3) and stirring for 30 min yielded an orange oil upon workup. TLC on alumina (eluting with CH_2Cl_2:MeOH, 95:5) revealed three products and a small amount of **1**. Band 1, crystallized from CH_2Cl_2, gave **7**. Anal. Calcd for $C_{54}H_{60}Cl_2Fe_2N_2P_2Pt_2 \cdot CH_2Cl_2$: C, 45.35; H, 4.30; N, 1.92. Found: C, 45.60; H, 4.40; N, 1.88. ^{1}H NMR ($CDCl_3$): 3.05 (m, 6H, NMe); 3.26 (m, 6H, NMe); 3.35, 3.40, 3.53, 3.57 (m, 4H, NC*H*$_2$). Conductivity (Λ_m, acetone): 0. Sodium triflate was added to a methanol solution of the product from band 2, **5a**; workup gave a red powder which crystallized from methanol/EtOAc to give **5b**. Anal. Calcd for $C_{42}H_{44}F_3FeNO_3P_2PtS$: C, 49.81; H, 4.38; N, 1.38. Found: C, 49.74; H, 4.76; N, 1.36. ^{1}H NMR ($CDCl_3$): 2.65 (m, 3H, NC*H*$_3$); 2.69 (m, 3H, NC*H*$_3$); 3.01 (m, 1H, η^5-C_5H_3); 3.18 (dd, 1H, NC*H*, J = 14.4, 3.7); 3.68 (d, 1H, NC*H*, J = 14.4 Hz). Conductivity (Λ_m, acetone): 140 Ω^{-1} mol^{-1} dm^2. Band 3 was obtained from methanol/EtOAc/CH_2Cl_2 as a red powder **9**. Anal. Calcd for $C_{41}H_{44}ClFeNP_2Pt \cdot CH_2Cl_2$: C, 51.26; H, 4.71; N, 1.42. Found: C, 51.53; H, 4.89; N, 1.73. ^{1}H NMR ($CDCl_3$): 2.78 (m, 6H, NMe).

***R,S*-{Pt[(η^5-C_5H_5)Fe(σ,η^5-$C_5H_3CH_2NMe_2$)]η^2-dppf}$^+X^-$ (6).** The addition of dppf (100 mg, 1.81×10^{-4} mol) to a solution of *R,S*-**1** (100 mg, 1.82×10^{-4} mol) in $CHCl_3$ (25 cm^3) caused a rapid color change to dark orange. The solvent was removed yielding a red oil **6a** (X = Cl). This oil was dissolved in minimum methanol, sodium triflate added, and the combined precipitate of NaCl and **6b** (X = CF_3SO_3) collected. Recrystallization of the precipitate from hot methanol yielded orange crystals of **6b** as a methanol solvate; yield 63%. Anal. Calcd for $C_{48}H_{44}F_3Fe_2NO_3P_2PtS \cdot CH_3OH$: C, 50.19; H, 4.13; F, 4.86; N, 1.19; S, 2.73. Found: C, 49.20; H, 3.90; N, 4.72; N, 1.20; S, 2.70. ^{1}H NMR ($CDCl_3$): 2.72 (m, 3H, ^3J(Pt−H) = 3 Hz, ^1J(H−H) = 1.5 Hz, NC*H*$_3$); 2.95 (m, 3H, ^3J(Pt−H) = 28 Hz, J(H−H) = 1.9 Hz, NC*H*$_3$); 3.28 (dd, 1H, J = 14.1, 4.8, NC*H*); 3.91 (d, 1H, J = 14.1, NC*H*). Conductivity (Λ_m, acetone): 154 Ω^{-1} mol^{-1} dm^2.

{Pt[(η^5-C_5H_5)Fe(σ,η^5-$C_5H_3CH_2NMe_2$)Cl]}$_x$dppbz (x = 1 (10), 2 (8)). *R,S*-**1** (80 mg, 1.45×10^{-4} mol) was dissolved in chloroform (25 cm^3) and dppbz (65 mg, 1.45×10^{-4} mol) added with stirring at room temperature. The solvent was removed and preparative TLC of the products on silica gel (ether) gave two yellow bands. Band 1 was recrystallized from hexane/EtOAc to give yellow crystals of **10**; yield 30 mg. Anal. Calcd for $C_{43}H_{40}ClFeNP_2Pt$: C, 56.19; H, 4.39; N, 1.52. Found: C, 56.51; H, 4.55; N, 1.20. ^{1}H NMR ($CDCl_3$): 3.12 (m, 3H, ^4J(P−H) = 3 Hz, ^3J(Pt−H) = 24 Hz, NC*H*$_3$); 3.36 (m, 3H, ^4J(P−H) = 3 Hz, ^3J(Pt−H) = 20 Hz, NC*H*$_3$); 3.65 (m, 3H, ^3J(Pt−H) = 25 Hz, NC*H*$_2$). Conductivity (Λ_m, acetone) = 4 Ω^{-1} mol^{-1} dm^2. **10** rapidly converts to **8** in all solvents. Band 2 crystallized from hexane/EtOAc to give 23 mg of **8**. Anal. Calcd for $C_{56}H_{56}Cl_2Fe_2N_2P_2Pt_2$: C, 48.33; H, 4.06; N, 2.01. Found: C, 48.57; H, 4.14; N, 1.61. ^{1}H NMR ($CDCl_3$): 3.10 (6H, NC*H*$_3$); 3.34 (6H, NC*H*$_3$). Conductivity (Λ_m, acetone): 3 Ω^{-1} mol^{-1} dm^2.

Bppfa Complexes from 1. *R,S*-**1** (30.4 mg, 0.06 mmol) and bppfa (37 mg, 0.06 mmol) in chloroform (20 cm^3) were stirred for 5 min. The orange oil obtained by stripping the solvent was chromatographed on alumina (1:1, EtOAc:MeOH). The first band rapidly decomposed; TLC on silica showed the second band to be a mixture of products. Sodium triflate in MeOH was added to the oil from the second band, and a red precipitate formed. Recrystallization from MeOH/EtOAc gave a 42% yield of **12**α. Anal. Calcd for $C_{51}H_{51}F_3Fe_2N_2O_3P_2PtS$: C, 51.14; H, 4.29; N, 2.34. Found: C, 50.85; H, 4.10; N, 2.26. ^{1}H NMR ($CDCl_3$): 2.27 (s, 6H, CH_2NMe_2); 2.91 (m, 3H, NC*H*$_3$), 3.33 (dd, 1H, J = 14.2, 5.3 Hz, NC*H*); 3.34 (m, 3H, NC*H*$_3$); 3.81 (d, 1H, J = 14.2 Hz, NC*H*). Conductivity (Λ_m, acetone): 124 Ω^{-1} cm^{-1} dm^2. The residual orange solution was separated on neutral alumina (9:1 MeOH:EtOAc) into two components, **11**α and **11**β, and traces of **12**α and **12**β. ^{1}H NMR ($CDCl_3$) for **11**α/**11**β: 1.27, 1.29 (2H, NC*H*$_2$); 1.79 (6H, N*Me*$_2$); 3.22 (3H, NC*H*$_3$); 3.46 (3H, NC*H*$_3$). Both **11**α and **11**β rapidly converted to **12** on standing.

Separation of *meso*- and *dl*-Pt$_2$[(σ,η^5-$C_5H_3CH_2NMe_2$)$_2$Fe](dmso)$_2$Cl$_2$ (2). The mixture of isomers was prepared from (η^5-$C_5H_4CH_2NMe_2$)$_2$-Fe and $PtCl_2$(dmso)$_2$ as described in ref 5. After this mixture was refluxed for 2 h, CH_2Cl_2 was added to the methanol solution to dissolve the products and the solution filtered through a Celite pad to remove Pt residues. Solvents were removed, the residue redissolved in CH_2Cl_2, and ethyl acetate slowly added until the first crystals appeared. When this was allowed to stand, yellow crystals of *meso*-**2** were deposited. The first batch of crystals was collected and the ethyl acetate procedure repeated with seeding. Once the yellow isomer was separated (yield ~ 30%), the liquor was evaporated and the residue recrystallized from CH_2Cl_2/MeOH to afford fine orange crystals of *dl*-**2**; yield 15%. There are significant differences in the physicochemical properties of the two isomers. The *meso* isomer is more soluble in methanol, and it rapidly decomposes to green compounds in all solvents. The relative yield of isomers does not reflect the enantiomeric selectivity of the initial reaction, since the yellow *meso* isomer decomposes during workup and low yields of the *meso* isomer are not uncommon. Furthermore, although the stereoisomers can be chromatographically separated on silica gel only the *dl* isomer can be recovered (this procedure can also be used for the bromo analogue). Consequently, *dl*-**2** can be isolated by removing the decomposition products from a "decomposed" solution of both isomers, but it is then difficult to crystallize.

***meso*-{Pt$_2$[(σ,η^5-$C_5H_3CH_2NMe_2$)$_2$Fe](η^2-dppm)$_2$]}$^{2+}X^-_2$ (13).** *meso*-**2** (47 mg, 5.1×10^{-5} mol) and dppm (40 mg, 1.04×10^{-4} mol) were dissolved in chloroform (10 cm^3), and the mixture was stirred while the solution color turned deep-orange. The solvent was evaporated *in vacuo* to yield a red oil **13a** (X = Cl) which was dissolved in a minimum amount of MeOH and a solution of sodium triflate in MeOH added. After filtration, the solvent was removed to give a solid which was recrystallized from MeOH:EtOAc to give orange needles of **13b** (X = CF_3SO_3); yield 90%. **13b** is insoluble in ether and hexane, sparingly soluble in EtOAc, and soluble in alcohols. Anal. Calcd for $C_{68}H_{66}F_6FeN_2O_6P_4Pt_2S_2$: C, 46.53; H, 3.79; N, 1.60. Found: C, 46.18; H, 3.56; N, 1.55. ^{1}H NMR ($CDCl_3$): 2.62 (bs, 6H, C*H*$_3$N); 3.01 (bs, 6H, C*H*$_3$N); 3.13 (bs, 4H, C*H*$_2$N). Conductivity (Λ_m, acetone): 315 Ω^{-1} mol^{-1} dm^2. A similar reaction with *dl*-**2** gave *dl*-**13** as a red oil which resisted all attempts to crystallize it. Consequently, *meso*-**13b** can easily be obtained from unresolved **2** by carrying out the reaction of dppm with the crude reaction product from the preparation of **2**; on conversion to the triflate salt, *meso*-**13b** preferentially crystallizes in high yield leaving *dl*-**13** in solution.

***meso*-{Pt$_2$[(σ,η^5-$C_5H_3CH_2NMe_2$)$_2$Fe](η^2-dppe)$_2$}$^{2+}X^-_2$ (14).** *meso*-**2** (64 mg, 7×10^{-5} mol) and dppe (55.7 mg, 14×10^{-5} mol) were dissolved separately in chloroform (10 cm^3), and the solutions were mixed and stirred for 15 min during which a deepening of the orange color occurred. The solvent was removed in vacuo to yield a red solid/oil **14a** (X = Cl) which was dissolved in methanol and sodium triflate added. The orange precipitate was dissolved in hot CH_2Cl_2 to remove small amounts of white solid, and EtOAc added. Burnt orange crystals

Table 1. Crystallographic Data for **3b** and **13b**

	3b	**13b**
chem formula	$C_{39}H_{38}NO_3F_3SP_2FePt$	$C_{76}H_{74}N_2O_{10}F_6P_4S_2Cl_2FePt_2$
a, Å	12.755(2)	12.335(1)
b, Å	16.011(3)	16.102(1)
c, Å	18.710(3)	18.956(1)
α, deg	90	90
β, deg	90	98.82(7)
γ, deg	90	90
V, Å^3	3821(1)	3725.9(4)
Z	4	2
fw	970.66	1923.40
space group	$P2_12_12_1$ (No 19)	$P2_1/n$ (No. 14)
T, °C	183(5)	183(5)
λ, Å	0.710 69	0.710 69
ϱ_{calcd}, g cm^{-3}	1.687	1.714
μ(Mo Kα), cm^{-1}	42.26	41.54
transm coeff	0.601 (max), 0.268 (min)	0.778 (max), 0.487 (min)
R[a]	0.0443	0.0399
$R_w(F_o)$[b]	0.0457	
wR2(F_o^2)[c]		0.1078

[a] $R = [\sum|F_o| - |F_c|/\sum|F_o|]$ $[F > 2\sigma(F)]$. [b] $R_w(F_o) = [\sum w^{1/2}|F_o| - |F_c|/\sum w^{1/2}F_o|]$; $w = [1.0/(\sigma^2F_o + 0.004973F_o^2)]$. [c] wR2($F_o$) = $[\sum w(F_o^2 - F_c^2)^2/\sum wF_o^4]^{1/2}$ (all data); $w = [1/(\sigma^2F_o^2 + (0.0499P)^2) + 58.29P]$; $P = (\max F_o^2, 0 + 2F_c^2)/3$.

formed of **14b** (X = CF_3SO_3), which slowly lost the solvent of crystallization, causing cracking of the crystals; yield 60%. Anal. Calcd for $C_{70}H_{70}O_6F_6FeN_2P_4Pt_2S_2.CH_2Cl_2$: C, 45.65; H, 3.88; N, 1.49; S, 3.4. Found: C, 45.91; H, 3.89; N, 1.51; S, 3.6. ^{1}H NMR ($CDCl_3$): 2.71 (bs, 6H, CH_3N); 3.04 (bs, 6H, CH_3N). Conductivity (Λ_m, acetone): 295 Ω^{-1} mol^{-1} dm^2. The analysis of the reaction mixture shows that another product with higher R_f is present in small amounts which gives ^{31}P NMR ($CDCl_3$): 41.9 (^1J(Pt−P$_N$) = 3600 Hz) and 36.2 (^1J(Pt−P$_N$) = 3600 Hz).

***meso*-{Pt$_2$[(σ,η^5-C$_5$H$_3$CH$_2$NMe$_2$)$_2$Fe](η^2-dppf)$_2$}$^{2+}$X$^-_2$ (15).** *meso*-**2** (67 mg, 7.3 × 10^{-5} mol) and dppf (81 mg, 14.6 × 10^{-5} mol) were dissolved in chloroform, and the red solution was stirred for 15 min. Solvent was removed leaving a red oil, **15a** (X = Cl), which was dissolved in minimum amount of MeOH and sodium triflate added. The precipitate was removed, washed with EtOAc and the filtrate plus washings stripped *in vacuo*. The residue was columned on neutral alumina (acetonitrile) yielding one major band which was recrystallized from hot MeOH to give red crystals of **15b** (X = CF_3SO_3); yield 70%. Anal. Calcd for $C_{86}H_{78}F_6Fe_3N_2O_6P_4Pt_2S_2$: C, 49.30; H, 3.75; N, 1.34. Found: C, 49.01; H, 3.55; N, 1.32. ^{1}H NMR ($CDCl_3$): 2.65 (bs, 6H, CH_3N); 2.93 (bs, 6H, CH_3N). Conductivity (Λ_m, acetone): 309 Ω^{-1} mol^{-1} dm^2. *dl*-**15** was prepared by a similar procedure given for the preparation of the dppm complex except the reaction temperature was 35 °C. Yields were low as the *dl* complex proved to be unstable in solution. ^{1}H NMR ($CDCl_3$): 2.65 (bs, 6H, (NCH_3)$_2$); 2.93 (bs, 6H, (NCH_3)$_2$). ^{31}P NMR ($CDCl_3$): 20.5 (^1J(Pt−P$_C$) = 2010 Hz), 13.8 (^1J(Pt−P$_N$) = 3770 Hz).

X-ray Structure Analyses. Diffraction data were collected on a yellow, platelike crystal of **3b** and a deep red, block-shaped crystal of **13b** on a Nicolet R3M diffractometer at 183(5) K, using graphite monochromated Mo Kα radiation. The data were corrected for Lorentz and polarisation effects using SHELXTL.[13a] Analytical absorption corrections were applied to the data for **3b** using SHELX-76[13b] and empirical corrections applied to the data for **13b** using SHELXTL. Other details of the crystals, data collection and refinement are summarized in Table 1. Both structures were solved by Patterson methods using SHELXS-86[13c] with the chosen Fourier maps showing the location of the Pt, Fe, and P and a number of the other heavy atoms. For **13b**, the Fe atom is located on a crystallographic center of symmetry and was constrained appropriately in subsequent refinement. Weighted, full-matrix refinement of **3b** minimizing $\sum w(|F_o| - |F_c|)^2$[13d] was performed with an extended version of SHELX-76,[14] and refinement of **13b** on F_o^2 used SHELXL-93. The location of the remaining non-hydrogen atoms in the Pt complexes and the triflate anions was revealed in both cases by a series of difference Fourier, least-squares refinement cycles. Hydrogen atoms on the ferrocenylamine moieties and the phenyl rings of the phosphine ligands were included in calculated positions using a riding model (d(C−H) = 0.98 Å). For **3b** the final refinement converged with $R = 0.443$, $R_w = 0.0457$; an additional refinement with the sign of all the positional coordinates reversed converged with $R = 0.0674$, $R_w = 0.0739$, indicating that the handedness of the structure is correctly represented by the original coordinates. For **13b** a difference synthesis following the location of the non-hydrogen atoms revealed the presence of an ethylacetate molecule of crystallization. Inclusion of the additional atoms resulted in a significant improvement of the overall model. The solvate molecule displayed positional disorder in the acetate methyl group; refinement of the occupancy factors converged at 0.60(3) for C(41) and 0.40(3) for C(41A). High and increasing temperature factors together with the presence of a number of high Fourier peaks in the vicinity of the solvate molecule indicated the possibility of additional non-resolvable disorder, but this was not investigated further. Final positional and equivalent thermal parameters for **3b** and **13b** are given in Tables 2 and 3 respectively. Full tables of bond lengths and angles, thermal parameters and H-atom parameters are included in the deposited data.

Results and Discussion

Synthesis. Reactions of the platinocycle **1**, *R*,*S*-{Pt[(η^5-C$_5$H$_5$)Fe(σ,η^5-C$_5$H$_3$CH$_2$NMe$_2$)](dmso)Cl} with dppm, dppe, dppb, or dppf in chloroform occur rapidly to displace both coordinated Cl$^-$ and dmso to give the novel salts *R*,*S*-{Pt[(η^5-C$_5$H$_5$)Fe(σ,η^5-C$_5$H$_3$CH(R)NMe$_2$)](η^2-P-P)}$^+$X$^-$ (**3** − **6**), (eq 1). The chloride salts (**3a**−**6a**) tended to be hygroscopic and analytically pure crystalline salts were generally obtained with $CF_3SO_3^-$ as counterion (**3b**−**6b**).

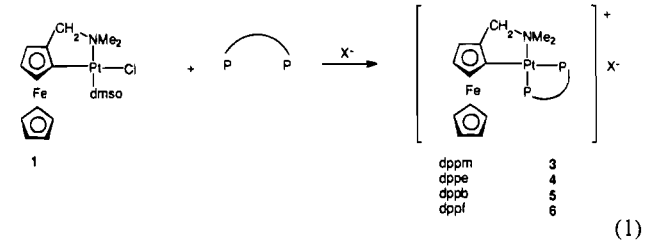

1 (1)

These salts had conductances in acetone typical of large 1:1 electrolytes and a PtN(σ-C)(η^2-P-P) coordination sphere was deduced from the spectroscopic data *(vide infra)*. Compounds **3**−**6** were insoluble in hexane, benzene, and ethers, slightly soluble in water, but readily soluble in alcohols, halogenated solvents, and dmso. In dmso and methanol/water solvents, with or without Cl$^-$ ion, the coordination sphere remains intact up to 50 °C which makes these salts ideal for biological testing.

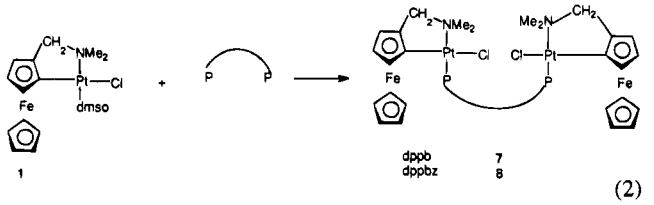

1 (2)

Dppb proved to be a flexible ligand as both μ-linked, **7**, and η^1-pendant, **9**, substitution products were isolated as minor

(13) (a) Sheldrick, G. M. SHELXTL, an integrated system for solving, refining and displaying crystal structures from diffraction data. University of Göttingen, 1981. (b) Sheldrick, G. M. SHELX-76, program for crystal structure determination. University of Cambridge 1981. (c) Sheldrick, G. M. SHELXS-86, program for the solution of crystal structures from diffraction data. University of Göttingen, 1986. (d) Sheldrick, G. M. SHELXL-93; FORTRAN-77 program for the refinement of crystal structures from diffraction data. University of Göttingen, 1993. *J. Appl. Crystallogr.*, in press.

(14) Rabinovich, D.; Reich, K., SHELXL400. A modification of SHELX-76 to allow the refinement of up to 400 atoms, Weizmann Institute of Science, Rehovot, Israel, 1979.

Table 2. Atomic Coordinates ($\times 10^4$) and Equivalent Isotropic Displacement Parameters ($Å^2 \times 10^3$) for **3b**

	x	y	z	$U(eq)^a$		x	y	z	$U(eq)^a$
Pt(1)	7959.0(4)	679.2(3)	4080.6(2)	21	C(24)	6484(12)	−2730(11)	4851(9)	48
N(1)	7482(9)	1520(7)	4944(6)	29	C(25)	7539(14)	−2826(9)	5082(9)	42
C(13)	8481(11)	1935(9)	5187(7)	32	C(26)	8194(11)	−2146(9)	5047(8)	37
C(14)	6983(13)	1064(9)	5559(6)	38	P(2)	8616(3)	−154(2)	3230(2)	24
C(1)	6720(10)	2205(8)	4670(7)	29	C(27)	9459(9)	−765(9)	3845(6)	29
C(2)	6815(9)	2233(8)	3869(6)	25	C(28)	7688(9)	−845(7)	2813(7)	26
C(3)	7283(10)	1548(9)	3471(6)	28	C(29)	6608(10)	−626(11)	2781(8)	39
C(4)	7124(12)	1750(8)	2716(7)	31	C(30)	5933(12)	−1216(9)	2481(9)	43
C(5)	6549(10)	2525(10)	2658(8)	36	C(31)	6242(11)	−1960(10)	2210(7)	37
C(6)	6370(10)	2849(10)	3390(8)	34	C(32)	7310(12)	−2194(8)	2242(7)	37
Fe(1)	7938(2)	2708(1)	3179(1)	28	C(33)	8023(12)	−1636(8)	2535(7)	32
C(8)	9104(11)	3376(8)	3709(8)	36	C(34)	9409(9)	296(8)	2532(5)	20
C(9)	9567(11)	2666(9)	3370(8)	36	C(35)	10410(10)	637(9)	2666(7)	30
C(10)	9316(11)	2730(9)	2612(8)	32	C(36)	10980(11)	1013(9)	2119(8)	40
C(11)	8727(11)	3492(9)	2496(8)	39	C(37)	10583(12)	1066(10)	1424(7)	36
C(12)	8592(12)	3889(8)	3171(9)	41	C(38)	9586(12)	734(11)	1280(7)	43
P(1)	8713(3)	−469(2)	4655(2)	24	C(39)	8991(13)	329(9)	1830(7)	36
C(15)	9602(9)	−441(8)	5415(7)	24	S(1)	7195(3)	5467(2)	1112(2)	36
C(16)	9376(11)	−808(9)	6089(7)	36	O(1)	7804(8)	4707(7)	1080(6)	48
C(17)	10078(12)	−751(10)	6643(7)	41	O(2)	6914(9)	5754(9)	1828(6)	67
C(18)	11043(13)	−333(10)	6561(8)	42	O(3)	7552(13)	6092(8)	627(10)	100
C(19)	11305(10)	22(9)	5886(8)	39	C(40)	5964(13)	5176(15)	762(12)	72
C(20)	10581(9)	−23(8)	5323(7)	26	F(1)	5250(11)	5772(12)	773(9)	138
C(21)	7844(10)	−1358(8)	4798(6)	24	F(2)	5508(11)	4563(11)	1144(11)	131
C(22)	6775(10)	−1288(8)	4576(8)	33	F(3)	6023(13)	4882(13)	95(7)	148
C(23)	6118(13)	−1992(10)	4598(9)	46					

[a] $U(eq)$ is defined as one-third of the trace of the orthogonalized U_{ij} tensor.

Table 3. Atomic Coordinates ($\times 10^4$) and Equivalent Isotropic Displacement Parameters ($Å^2 \times 10^3$) for **13b**

	x	y	z	$U(eq)^a$		x	y	z	$U(eq)^a$
Pt(1)	2581(1)	999(1)	74(1)	12(1)	C(28)	1189(6)	1850(5)	−1505(4)	14(2)
N(1)	2945(6)	417(4)	1111(3)	17(2)	C(29)	593(7)	1277(5)	−1964(4)	16(2)
C(13)	3903(7)	−123(6)	1039(4)	22(2)	C(30)	−473(7)	1449(6)	−2278(4)	21(2)
C(14)	3232(6)	948(5)	1734(3)	22(2)	C(31)	−938(7)	2218(6)	−2157(4)	25(2)
C(1)	1999(5)	−134(4)	1235(3)	15(2)	C(32)	−336(7)	2797(6)	−1727(5)	25(2)
C(2)	1451(6)	−448(5)	518(4)	12(2)	C(33)	724(7)	2613(5)	−1395(4)	21(2)
C(3)	1639(6)	−24(5)	−111(4)	13(2)	C(34)	3148(6)	962(5)	−1647(4)	15(2)
C(4)	974(6)	−446(5)	−692(4)	14(2)	C(35)	3577(6)	1376(6)	−2178(4)	19(2)
C(5)	408(6)	−1121(5)	−415(4)	14(2)	C(37)	4035(7)	88(6)	−2688(4)	26(2)
C(6)	706(6)	−1118(5)	340(4)	16(2)	C(38)	3598(7)	−343(6)	−2164(5)	25(2)
Fe(1)	0	0	0	11(1)	C(39)	3159(7)	85(5)	−1627(4)	20(2)
P(1)	3540(2)	2235(1)	211(1)	14(1)	O(1)	−853(6)	1638(5)	2682(4)	40(2)
C(15)	2992(7)	3106(5)	645(4)	18(2)	O(2)	476(6)	586(4)	2549(4)	39(2)
C(16)	2148(7)	2979(6)	1047(4)	22(2)	O(3)	592(8)	1938(5)	1992(4)	57(2)
C(17)	1765(8)	3633(7)	1404(5)	34(2)	S(1)	230(2)	1455(2)	2547(1)	28(1)
C(18)	2205(9)	4416(7)	1363(5)	35(2)	C(40)	1097(8)	1841(6)	3341(5)	28(2)
C(19)	3031(9)	4548(6)	963(6)	39(2)	F(1)	1050(5)	2664(3)	3394(3)	42(2)
C(20)	3419(8)	3896(6)	614(5)	32(2)	F(2)	799(5)	1532(4)	3939(3)	40(2)
C(21)	5004(6)	2267(5)	530(4)	16(2)	F(3)	2140(5)	1624(4)	3349(4)	49(2)
C(22)	5743(7)	1936(6)	125(4)	23(2)	C(41)	1355(11)	161(10)	−3827(8)	30(5)
C(23)	6857(7)	1891(6)	384(5)	30(2)	C(41A)	1620(17)	−634(13)	−3754(10)	14(7)
C(24)	7224(8)	2185(6)	1080(5)	27(2)	C(42)	2304(24)	−24(11)	−4123(12)	182(10)
C(25)	6504(7)	2516(6)	1480(5)	26(2)	O(4)	2990(15)	−677(9)	−4184(9)	139(7)
C(26)	5387(7)	2554(6)	1216(4)	22(2)	O(5)	2881(15)	679(9)	−4420(9)	140(6)
C(27)	3332(7)	2471(5)	−758(4)	19(2)	C(43)	4043(14)	665(12)	−4712(8)	77(5)
C(36)	4031(6)	933(6)	−2694(4)	24(2)	C(44)	4167(19)	1522(14)	−4937(10)	110(7)
P(2)	2493(2)	1536(1)	−1012(1)	13(1)					

[a] $U(eq)$ is defined as one-third of the trace of the orthogonalized U_{ij} tensor.

components from the reaction of this ligand with **1** (eqs 2 and 3) in addition to the η^2 chelate **5**. During reactions of **1** with dppb, concurrent oxidation of the uncoordinated ligand to dppbO occurred readily but none of the isolated products had the characteristic (P=O) bands around 1200 cm^{-1} or low-field ^{31}P resonances of a phosphoryl complex; this was not a problem with the other ligands. However, once coordinated, oxidation of the pendant phosphorus did not take place so it is likely that a metal-catalyzed ligand oxidation process is involved. ^{31}P NMR evidence was obtained for a η^1-dppf derivative, but like **9**, it rapidly converted to a η^2 chelate on workup; this facile ring closure is presumably the reason why no NMR evidence was found for a η^1-dppe or dppm analogue. In contrast, the bridged complexes showed no tendency to rearrange to chelate products.

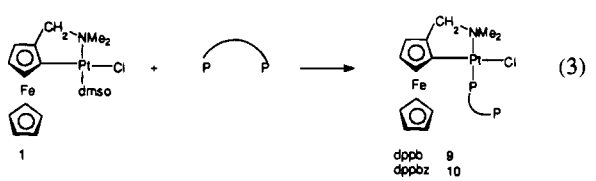

(3)

Complex **8**, in which dppbz provides a rigid link between the Pt(II) moieties, was the major product from the reaction

with **1**, although a labile pendant representative **10** was obtained as the minor product.

R,S-{Pt[(η^5-C_5H_5)Fe(σ,η^5-$C_5H_3CH_2NMe_2$)](η^1-bppfa)Cl} (**11**) with both pendant CH_2NMe_2 and PPh_2 groups and *R,S*-{Pt[(η^5-C_5H_3)Fe(σ,η^5-$C_5H_3CH_2NMe_2$)](η^2-bppfa)}$^+X^-$ (**12**) with a pendant CH_2NMe_2 were obtained by reaction of **1** with bppfa (eq 4). Two isomers of **12** were identified spectroscopically in the crude reaction product, differing in their mode of attachment of bppfa to the Pt(II) coordination sphere; **12α** had the $PPh_2(C_5H_3CH_2NMe_2)$ and **12β** the $PPh_2(C_5H_4)$ ring *trans* to the Pt−N bond, respectively. Only **12α**, the predominant isomer, was obtained as a crystalline product. Two isomers, **11α** and **11β** were also isolated, but because of the lability of these η^1 derivatives, analytically pure samples were not obtained. These mixed ferrocenylamine complexes offer a useful template for the synthesis of heterometallic derivatives and will allow the cytotoxic activity of compounds with both coordinated and pendant amine functionality to be explored.

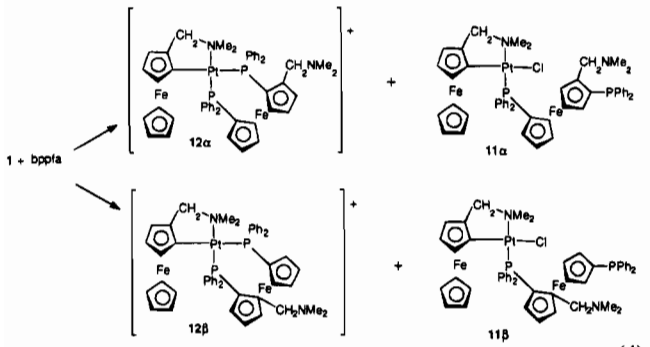

(4)

Cyclometalation of *trans*-{Pt_2[Fe(η^5-$C_5H_4CH_2NMe_2$)$_2$]X_2-(dmso)$_2$} gave both *meso* and *dl* enantiometric configurations of the diplatinum platinocycle **2**. Since antiproliferative activity could depend on the stereochemistry of the complex, a method

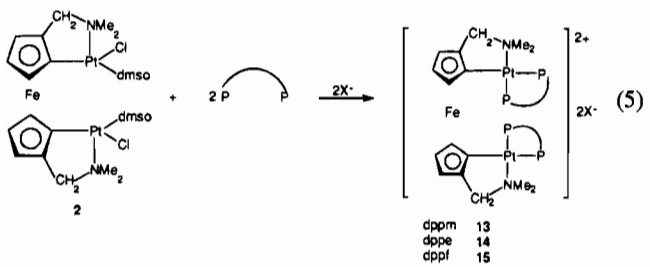

(5)

was developed for the separation of *meso*- and *dl*-**2** (see Experimental Section). Substitution reactions (eq 5) using either *meso*- or *dl*-platinocycle **2** provided a sequence of diplatinum chelate derivatives *meso*- or *dl*-{Pt_2[(σ,η^5-$C_5H_3CH_2NMe_2$)$_2$Fe]-(η^2-P-P)}$^{2+}X^-_2$ (**13**−**15**). There was a marked decrease in the oxidative stability of bis(platinocycles) **13**−**15** compared to the monoplatinum analogues as has been noted previously.[5] A further subtlety is that the oxidative stability in solution of *dl*-**13**−**15** is much less than *meso*-**13**−**15**—the converse of the relative stability of unsubstituted *dl*- and *meso*-**2** (see Experimental Section)—and therefore most of the discussion in this paper will concern the *meso* complexes. Because of the variety of coordination modes found in the monoplatinum dppb and bppfa complexes, reactions of these ligands with **2** were not attempted.

Cyclometalation of *cis*-{Pt[(η^5-C_5H_5)Fe(η^5-$C_5H_4CH_2NMe_2$)]-Cl(η^2-P-P)}$^+$ conceptually provides an alternative route to the derivatives above. Stereochemical constraints imposed on the electrophilic attack and the elimination of HX in the cyclometalation reaction by the chelated phosphine ligand could provide some degree of enantiomeric selectivity. However, even under the mildest reaction conditions, the bidentate ligands displaced both the ferrocenylamine and dmso from *trans*-{Pt[(η^5-C_5H_5)Fe(η^5-$C_5H_4CH_2NMe_2$)]Cl_2(dmso) to give *cis*-Pt(η^2-P-P)-Cl_2.[15] Substitution of dmso by the phosphine occurs initially but, because of strong *trans* influence of the coordinated phosphine, ferrocenylamine loss and stereochemical rearrangement rather than electrophilic attack at the Cp ring was preferred.

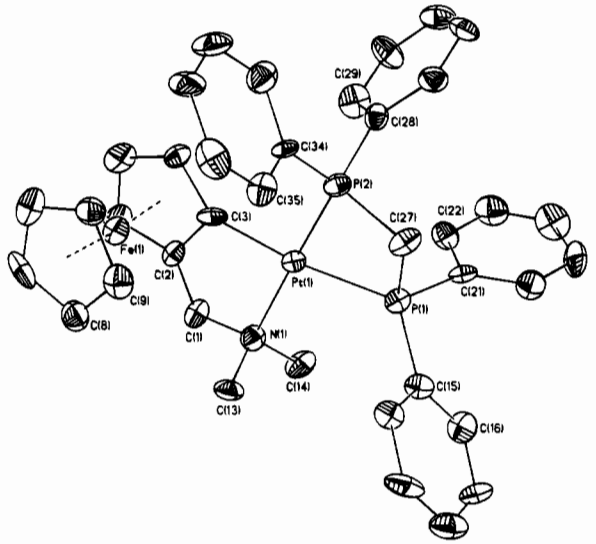

Figure 1. Molecular structure of the cation *S*-{Pt[(η^5-C_5H_5)Fe(σ,η^5-$C_5H_3CH_2NMe_2$)]dppm}$^+$, **3b**, showing the atom numbering scheme. Thermal ellipsoids are drawn at the 50% probability level. For clarity hydrogen atoms have been omitted and only the first two atoms of the consecutively numbered cyclopentadiene and phenyl rings have been labeled.

Characterization of Complexes. Complexes **3**−**10** and **12**−**15** were fully characterized by analysis, NMR, and IR spectra; the solid-state structures of the dppm complexes 3b and 13b were also determined. Characterization of 11 rests on the spectroscopic data.

X-ray Structures of 3b and 13b. Both compounds consist of well-separated cations and anions in the solid state with no intermolecular contacts not involving hydrogen atoms at less that 3.00 Å for **3b** and the shortest non-hydrogen atom contact for **13b** being 2.87(2) Å between O(1) and C(41A). General views of **3b** and **13b** which define the atom numbering scheme are shown in Figures 1 and 2, respectively. Selected bond lengths and angles for both molecules are given in Table 4.

Figure 1 shows the crystallographically determined *S* planar configuration for **3b**. In contrast, **13b** has the Fe atom located at a crystallographic center of symmetry (Figure 2) which identifies the cation as the *meso* stereoisomer. The two structures show considerable similarities. The close comparison between the coordination spheres of the Pt(II) atoms in both **3b** and **13b** undoubtedly reflects the fact that the *meso* configuration of **13b** results in a transoid relationship of the Pt atoms and their ligand moieties with respect to the cyclopentadiene rings. In this orientation no significant intramolecular interactions can occur to influence the coordination environment.[4] In each case the Pt(II) atoms are coordinated to the amine N(1) atoms, the metalated C(3) atoms of the ferrocenylamine ligands and to the two P atoms of the chelating bidentate dppm ligands. The coordination sphere of the Pt(1) atoms is severely distorted in both cations, with the N(1) and C(3) atoms forced out of the ligand plane by 0.18(1) and 0.13(1) Å

(15) Troitskaya, L. L.; Sokolov,V. I. *J. Organomet. Chem.* **1987**, *328*, 169.
(16) Braterman, P. S.; Cross, R. J.; Manjlovic-Muir, L.; Muir, K. W.; Young, G. B. *J. Organomet. Chem.* **1975**, *84*, C40.

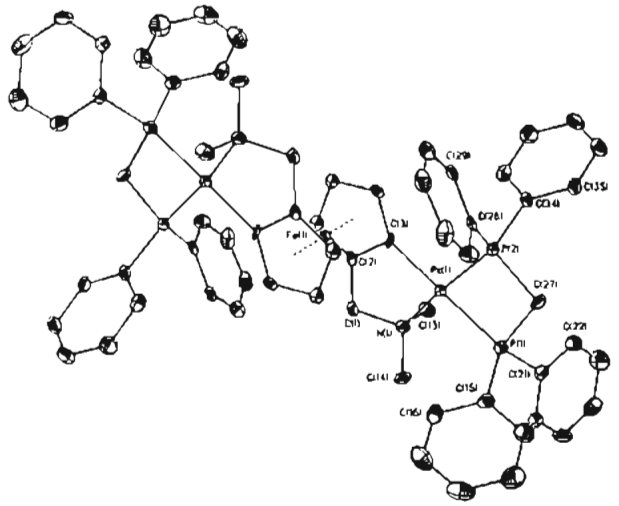

Figure 2. Molecular structure of *meso*-{$Pt_2[(\sigma,\eta^5\text{-}C_5H_3CH_2NMe_2)_2]$-$Fe(dppm)_2$}$^{2+}$ **13b**, showing the atom numbering scheme. Thermal ellipsoids are drawn at the 50% probability level. For clarity hydrogen atoms have been omitted, and only the first two atoms of the consecutively numbered cyclopentadiene and phenyl rings have been labeled.

Table 4. Selected Bond Lengths and Bond Angles for **3b** and **13b**

	3b	**13b**
	Bond Lengths (Å)	
Pt(1)−N(1)	2.19(1)	2.162(6)
Pt(1)−C(3)	2.00(1)	2.016(8)
Pt(1)−P(1)	2.337(3)	2.310(2)
Pt(1)−P(2)	2.239(3)	2.220(2)
N(1)−C(13)	1.51(2)	1.491(11)
N(1)−C(14)	1.50(2)	1.457(8)
N(1)−C(1)	1.55(2)	1.514(9)
C(1)−C(2)	1.50(2)	1.510(9)
C(2)−C(3)	1.45(2)	1.425(10)
C(2)−C(6)	1.45(2)	1.425(11)
C(3)−C(4)	1.46(2)	1.438(10)
C(4)−C(5)	1.45(2)	1.435(11)
C(5)−C(6)	1.48(2)	1.423(11)
C(8)−C(9)	1.43(2)	
C(8)−C(12)	1.45(2)	
C(9)−C(10)	1.46(2)	
C(10)−C(11)	1.45(2)	
C(11)−C(12)	1.42(2)	
P(1)−C(15)	1.82(1)	1.809(9)
P(1)−C(21)	1.82(1)	1.817(8)
P(1)−C(27)	1.85(1)	1.856(8)
P(2)−C(27)	1.85(1)	1.848(8)
P(2)−C(28)	1.80(1)	1.807(8)
P(2)−C(34)	1.80(1)	1.805(8)
	Bond Angles (deg)	
N(1)−Pt(1)−C(3)	82.7(5)	80.7(3)
N(1)−Pt(1)−P(1)	105.0(3)	103.9(2)
N(1)−Pt(1)−P(2)	174.1(3)	170.3(2)
C(3)−Pt(1)−P(1)	171.7(4)	174.7(2)
C(3)−Pt(1)−P(2)	99.9(4)	102.2(2)
P(1)−Pt(1)−P(2)	72.8(1)	73.75(7)
Pt(1)−N(1)−C(13)	105.0(7)	103.1(5)
Pt(1)−N(1)−C(14)	112.5(8)	118.2(5)
Pt(1)−N(1)−C(1)	111.5(8)	109.7(4)
N(1)−C(1)−C(2)	107(1)	107.9(5)
C(1)−C(2)−C(3)	121(1)	119.0(6)
Pt(1)−C(3)−C(2)	114.3(8)	114.2(5)
Pt(1)−P(1)−C(15)	126.6(4)	119.8(3)
Pt(1)−P(1)−C(21)	115.5(4)	122.0(3)
Pt(1)−P(1)−C(27)	92.1(4)	94.2(3)
Pt(1)−P(2)−C(27)	95.2(4)	97.5(3)
Pt(1)−P(2)−C(28)	115.4(4)	120.2(3)
Pt(1)−P(2)−C(34)	119.1(4)	117.1(3)

respectively for **3b** and by 0.242(7)Å and 0.193(7)Å for **13b** to opposite sides of the ligand meanplane. The Pt(1) atoms also lie above the mean planes by 0.033(1)Å in **3b** and 0.074(1)Å in **13b**. These distortions are likely to arise from the steric consequences of the dppm coordination. The P(1)−Pt(1)−P(2) angles are 72.8(1)° for **3b** and 73.75(7)° for **13b**, and other angles subtended at the Pt(1) centers reflect the particularly narrow bite of the dppm ligands. The Pt(1)−N(1), 2.19(1) and 2.162(6)Å, and Pt(1)−C(3), 2.00(1) and 2.016(8) Å for **3b** and **13b** respectively, distances do not differ significantly from those observed[4,5] in the parent complexes, **1** and *dl*-**2**. The Pt(1)−P(1) bonds, 2.337(3) Å for **3b** and 2.310(2) Å for **13b**, *trans* to the metalated C(3) atoms of the ferrocenylamine ligands, are significantly longer than Pt(1)−P(2), 2.239(3) and 2.220(2) Å. This disparity results from the considerable *trans* influence of the σ-bound C(3) atoms. The Pt(1)−P(1) bond lengths are similar to the mean value of 2.30(1) Å for the Pt−P vector, reported for the complex *cis*-[$PtPh_2$dppm].[17] The methylene C atom of the dppm ligand lies 0.53(1) Å below the PtL_4 mean plane in the direction of the Fe(1) atom for **3b**. In contrast, the corresponding atom in **13b** is displaced by 0.103(8) Å in the opposite direction. Other bond lengths and angles in the ferrocenyl ligands for both cations are unremarkable; for **3b** the cyclopentadiene rings are inclined at an angle of 6.9(5)° while for the centrosymmetric **13b** the rings are strictly parallel.

Interpretation of Spectroscopic Data. Selected data are given in Table 5; complete data are given in the deposited material. Assignments for the ^{1}H NMR were supported by appropriate 2-D spectra. The phosphorus atoms *trans* to the amine and the σ-PtC bonds are designated as P_N and P_C respectively. To facilitate the interpretation of the spectroscopic data *meso*-{$Pt_2[Fe(\sigma,\eta^5\text{-}C_5H_3CH_2NMe_2)_2](PPh_3)_2Cl_2$}, **17**, was prepared using the same procedure as that for the previously described[5] *dl*-**17**; the monoplatinum analogue *R,S*-{$Pt[(\eta^5\text{-}C_5H_5)Fe(\sigma,\eta^5\text{-}C_5H_3CH_2NMe_2)](PPh_3)Cl$} **16**[4], was also used as an acyclic reference.

η^2 Complexes. ^{1}H and ^{13}C spectra were consistent with the Pt(II) coordination sphere consisting of *trans* amine/P_N and *trans* σ-PtC/P_C groups, which was found in the solid-state structures of the dppm derivatives.

With the exception of **12**, the out-of-plane and interplane (with respect to the plane of chirality[17]) N*Me* and N*CH*$_2$ signals in the ^{1}H NMR can be differentiated, as was found[4,5] for **1** and **2**. The interplane NMe resonance is the downfield component, but the comparable N*CH*$_2$ resonance is the upfield component. Thus, in **6** there is one symmetrical N*CH* AB resonance whereas the other component is unsymmetrical with an additional ^{1}H coupling of 5 Hz; 2-D spectra do not allow a specific description of the interaction but since **3**−**5** and **12** also show a similar pattern, it is likely that this interaction involves the stereochemically active interplane NCH proton. Substitution of dmso and Cl^- by an η^2 P-P ligand has no marked effect on the ^{1}H chemical shift of the NMe groups and the distinction between the *meso* and *dl* sets of NMe resonances in diplatinum derivatives, which was described[5] for **2**, is still valid. An "odd" feature of the ^{1}H NMR was the coalescence of NMe resonances for the chloride salt of **4** whereas those for **4b** were "normal". Anion−cation interaction via an ion pair could explain this oddity, and this will be further studied by electrochemical techniques. In general, there is a progressive upfield shift in the ^{1}H resonances of the ferrocenyl ring and CH_2 from **1** or **2** to mono- to a diplatinum complexes attributable to the increasing cation charge. One of the ferrocenylamine metallocene resonances appears much further upfield than the other two—it reaches 2.73 ppm in **15**!—and it is assigned to an α proton which lies over the platinum coordination sphere. A similar, albeit smaller,

(17) (a) Butler, I. R.; Cullen, W. R.; Herring, F. G.; Jagannathan, N. R. *Can. J. Chem.* **1986**, *64*, 667. (b) Hayashi, T.; Yamamoto, A.; Ito, Y. *J. Chem. Soc., Chem. Commun.* **1989**, 495.

Table 5. ^{31}P and ^{195}Pt NMR Data for Phosphine Derivatives[a]

complex	ligand	δ_P(C) or δ_{P*}[b]	δ_P(N)	$^1J(P_C-Pt)$	$^1J(P_N-Pt)$	$^2J(P-P)$	δ_{Pt}	Δ_R[c]
			Monoplatinum Complexes					
3	dppm	−22	−32.2	1510	3300	40	−3970	−49
4	dppe	52.6	37.2	1964	3666	0	−4577	20
5	dppf	26	11.5	2120	4033	17.7	−4408	−6
6	dppb	23.8	10.1	1960	3820	20	−4390	−7
7	dppb		10.2		4230	0	−4015	
8	dppbz		17.2		4303	0	−4182	
9	dppb	−4.9	10.2		4240	0	−4019	
10	dppbz	−5	17		4300	0	−4188	
11α	bppfa	−23.0	5.9		4300	0	−4110	
11β	bppfa	−17.0	6.0		4333	0	−4081	
12α	bppfa	23.2	11.2	2104	3970	16	−4401	−6
12β	bppfa	28.7	8.7	2092	4060	–	–	−8
16	PPh_3		17.3		4287		−4173	
			Diplatinum Complexes					
meso-**13**	dppm	−23.1	−33.7	1519	3298	42.4	−3952	−51
dl-**13**	dppm	−22.2	−33	1510	3283	40	−3973	−50
meso-**14**	dppe	52.6	36.2	1960	3660	0	−4600	19
meso-**15**	dppf	26.3	11.3	2100	3990	17.3	−4409	−6
dl-**15**	dppf	20.5	13.8	2010	3770	–	–	−3
meso-**17**	PPh_3		14.9		3664		–	
dl-**17**	PPh_3		16.8		4295		−4117	

[a] Full spectroscopic data are given in the supplementary material; all data refers to the triflate salts. Coupling constants in Hz. [b] P* refers to the uncoordinated phosphorus. [c] Based on the δ_P(N) compared to that of **16**.

upfield shift was seen in the ^1H NMR of some naphthylferrocene compounds.[18] ^1H resonances for the dppe complex **14** were very broad at 25 °C but line widths decreased with decreasing temperature. Variable temperature behavior of the CH_2N and some Cp ring ^1H resonances in **2** was attributed[5] to the flipping of the CH_2 groups between the two orientations possible with respect to the plane of chirality. Exactly the same temperature dependence of the CH_2N and the Cp proton not adjacent to a coordinate bond was observed for **14**, but not **13** and **15**, so the fluxionality must be hindered by the comparative rigidity of the dppm and dppf chelate rings.

^{195}Pt NMR chemical shifts (Table 5) for **3**−**6** and **12**−**15** were in the expected[19] range for a Pt(P-P)(σ-C)(N) donor set; they were virtually identical for comparable mono- and diplatinum derivatives—e.g. **3b** (−3970) and **13b** (−3952). Because Cl^- in **1** and **2** has been substituted by a better σ-donor and π-acceptor, $^3J(Pt-H)$ becomes so small in the chelate complexes that it is unresolved, in contrast to the η^1 complexes where Cl^- is still coordinated and $^3J(Pt-H)$ is of similar magnitude to that for **1**. A $^1J(Pt-P_C)$ value of 1520 Hz is characteristic of a phosphorus atom *trans* to a σ-alkyl or σ-aryl substituent with a high *trans* influence and $^1J(Pt-P_N)$ = 3314 Hz typical of a platinum-bound phosphorus atom *trans* to an amine donor.[20] ^{31}P chemical shifts for the chelate complexes cover a wide range due to ring size and ring current effects as discussed below while the ^2J(P-P) coupling constants of ~39 Hz are compatible with a mutually *cis* arrangement for the phosphorus atoms.[21] The upfield component of the AB pattern is readily assigned (Table 5) to the phosphorus *trans* to the NMe_2 group by comparison with data for **17** and **18**. This suggests that the *trans* effect of the Pt−C bond pulls electron density from the Pt−P bond onto the ferrocenyl moiety. Despite the big variation in the stereochemical environment experienced by the Pt(II) and η^2-P-P ligands in the *meso* and *dl* stereoisomers of **13**−**15** there was no significant difference between the ^{195}Pt or ^{31}P chemical shifts, or $^1J(Pt-P)$ coupling constants indicating that chelate ring formation does not significantly increase inter-ring proximal effects.

Bppfa can form a P-P ring in two different configurations. Two isomers of the η^2-bppfa complex, *R*,*S*-**12**, were identified by $^{31}P\{^1H\}$ NMR in the reaction solution but only one was obtained as a crystalline product. Separate ^1H resonances for *each* NCH_3, CH_2, and Cp proton of the platinocycle and the bppfa ligand were seen for *R* and *S* configurations, and because of the complexity of the ^1H NMR, spectra have not been completely assigned. The ^1H resonance for the pendant $CH_2N(CH_3)_2$ occurs downfield by 0.5 ppm from the position in uncoordinated bppfa as a consequence of chelation. Coupling constants $^1J(Pt-P)$ (Table 5) and the ^{195}Pt chemical shift is similar to those for the dppf complex **6** and confirm that a P-P rather than P−N chelate is formed. An assignment of stereochemistry as *R*,*S*-**12α** rests on the $^{31}P\{^1H\}$ data but it is not unequivocal. The resonance at 11.2 ppm, corresponding to the phosphorus *trans* to the Pt−N bond, is virtually identical to that for **6** and this suggests that the PPh_2 has a similar coordination environment in the two derivatives. Furthermore, the equivalent resonance in the other isomer is upfield as expected if the PPh_2 is *ortho* to the amino group. If this assignment is correct then there is a different coordinative attachment in the major η^2 and η^1 kinetically preferred products (see below).

η^1 and Linked Complexes. For the linked and η^1 complexes **7**−**11** where only substitution of the dmso in **1** has occurred the Pt(P)(σ-C)(N)(Cl) donor set gives rise to ^1H and ^{195}Pt NMR data which, as expected, are similar to those for **16** and **17** and are not discussed further except to note that the out-of-plane NMe resonance in **8** and **10** moves downfield by ~0.25 ppm due to the proximity of the 1,4-disubstituted aromatic ring of the ligand. Both isomers of **11**, which have a pendant PPh_2 and $CH_2N(CH_3)_2$ substituents, displayed a high field ^1H or ^{31}P resonance with a chemical shift similar to those in the uncoordinated ligand; charge distribution across the alkyl chain or Cp ring is therefore negligible. The lability of **11** precluded detailed spectroscopic studies, so the assignment of stereochemistry rests on the $^{31}P\{^1H\}$ and ^{195}Pt NMR. Two AB doublets in the ^{195}Pt NMR, the major species at −4110 ($^1J(Pt-P_N)$ = 4300 Hz) and the other at −4081 ($^1J(Pt-P_N)$ = 4333 Hz),

(18) Foxman, B. M.; Rosenblum, M.; Sokolov, S.; Khrushchova, N. *Organometallics* **1993**, *12*, 4805.
(19) Pregosin, P. S. *Coord. Chem. Rev.* **1982**, *44*, 247.
(20) Pregosin, P. E.; Kunz, R. W. *^{31}P and ^{13}C NMR of TM Phosphine Complexes*; Springer-Verlag: Berlin, 1979.
(21) Mather, G. G.; Rapsey, J. N.; Pidcock, A. *Inorg. Nucl. Chem. Lett.* **1973**, *9*, 567.

confirm that bppfa is η^1 coordinated via a PPh_2 group. ^{31}P chemical shifts for the major isomer were 5.90 (J(Pt−P) = 4290 Hz) and −23.00 ppm; the absence of the resonance at −16.9 ppm shows that it is the PPh_2 in the same ring as the pendant amino group which is *trans* to the Pt−N bond in **11**β. Note that it is apparently the other isomer **11**α which cyclizes to the major η^2 product, **12**α.

Effect of Ring Size on ^{31}P and ^{195}Pt Parameters. Correlations between ring size and ^{31}P NMR parameters have been proposed for a number of systems based on the "ring contribution", Δ_R, to the chemical shift.[22] This ring contribution causes deviation in the ^{31}P chemical shift from the standard correlation for the coordination chemical shift, Δ, expressed in the relationship, $\Delta = A\delta + B$, where A and B are constants and δ is the shift for the free ligand. The theoretical basis for Δ_R is unclear, but in general 4-membered rings give a large negative (shielding), with 5-membered being a large positive, 6-membered a small negative, and 7-membered a small positive component, respectively, to the ^{31}P chemical shift. Therefore, shielding of the ^{31}P nucleus should decrease in the order dppm > dppf, bppfa > dppb > dppe, and this indeed is the order of the chemical shifts for **3**−**6** and **12**−**15** although values for dppf and dppb are very similar. *cis*-Disubstituted monodentate analogues of these chelates are unavailable so Δ_R was estimated by comparison with **17**, using as a basis the ^{31}P chemical shift *trans* or *cis* to the Pt−N bond (Table 5). Values of Δ_R for these ferrocenylamine complexes compare remarkably well with those for the complexes[23] [$PtMe_2$(P-P)] (P-P: Δ_R = −52 (dppm), 24 (dppe), −1 (dppb)). Values of Δ_R for the dppf ligand are not available, but it can be derived by comparing data for [$PtCl_2$(dppf)][6] and [$PtCl_2(PPh_3)_2$];[24] which gives Δ_R = −1. As expected Δ_R for bppfa is similar to that for dppf in the platinocycle complexes. It is significant that Δ_R does not depend upon the number of Pt(II) moieties per ferrocenylamine, confirming that the two coordination spheres are independent and are not influenced by intramolecular contacts caused by coordination of a chelate phosphine.

Relationships between chelation and ^1J(Pt−P) are often tenuous although coupling constants for 4-membered rings are generally smaller than those for larger rings and acyclic compounds.[22] This statement is also true for the chelate derivatives **3**−**6** (Table 5) where there is a difference of 350 Hz between the dppm and dppe complexes and a trend dppe < dppb < dppf ≃ bppfa < dppm, which as a group are separated by 250 Hz from acyclic complexes.[4] Consequently, the magnitude of ^1J(Pt−P) can be used for the determination of ring size. A similar pattern emerges for the diplatinum derivatives (Table 2), whether *meso* or *dl*. It is interesting that ^1J(Pt−P) for *the* acyclic *meso*- and *dl*-**17** differ by 600 Hz. Small ^2J(P−P) coupling constants are usual for complexes in which the phosphorus atoms occupy mutually *cis* (i.e. AB type)[20] positions. Contributions to ^2J(P−P) can accrue from through-the-backbone and/or through-the-metal J(P−P) and since Karplus-type angular dependence terms will be greatest for the strained four-membered rings, dppm complexes should have the largest ^2J(P−P) in a system where the metal and other ligands in the coordination sphere are constant. This is not always the case however; ^2J(P−P) for six-membered ring complexes can be greater than four-membered[24] and ^2J(P−P) for five-membered ring complexes greater than either six or seven-membered rings.[25] Decisive differences with ring size in ^2J(P−P) were noted for complexes **3**−**6** and **13**−**15** (Table 5). The most significant observation was that ^2J(P−P) was zero for *odd*-membered rings.

Conclusion

This work illustrates the flexibility of the Pt(II) coordination sphere once a ferrocenylamine is cyclometalated. Depending on the bite angle and conformational requirements of a bidentate phosphine ligand, complexes can be synthesized in which either one or two coordination sites are occupied by the phosphine ligand. Given that the phosphorus atom *trans* to the Pt−N bond will be exerting a strong *trans* influence it is conceivable that the Pt−N bond may now be labilized. This uncoordinated $-NMe_2$ or the pendant PPh_2 or CH_2NMe_2 in complexes **9**−**12** can be used as building blocks for the synthesis of hetero- or homopolymetallic compounds with the platinocycle as ligands. These compounds are described in another paper.[26]

Testing of the biological activity of complexes **3**−**6** and **12**−**15** is currently underway. A significant advantage of these ionic derivatives is that they provide a route to water-soluble compounds by the use of carboxylate counterions, with consequent efficiencies in pharmokinetic properties. Furthermore, it has been found[27] that their redox properties are solvent-dependent and vary with the number of Pt(II) ions coordinated per ferrocenyl ligand. This difference in stability with Pt(II) multiplicity as far as oxidation to ferrocenium derivatives is concerned was more obvious with the chelate phosphine complexes than the parent **1** and **2**, presumably due to the increased electron density in the HOMO orbital of the ferrocenylamine moiety. Transmission of electronic effects through to the ferrocene redox center is facilitated by cyclometalation. In the case of the diplatinum complexes the question of through-space interactions has been raised[5] but the structural and spectroscopic data for *meso*- or *dl*-**13**−**15** indicate that coordination of the phosphine ligand does not lead to increased intramolecular contacts. A detailed investigation of these effects, and the ramifications for the use of these complexes as radiation sensitisers will be discussed elsewhere.[26]

Acknowledgment. We thank Prof. Ward T. Robinson, University of Canterbury, for the use of diffractometer facilities and Dr. R. Ranatunge-Bandarage for preliminary experiments.

Supplementary Material Available: Tables of crystallographic data, bond length and angle data, anisotropic thermal parameters, hydrogen positional and thermal parameters, and analytical and spectroscopic data (16 pages). Ordering information is given on any current masthead page.

(22) Garrou, P. E.; *Chem. Rev.* **1981**, *81*, 229.
(23) Appleton, T. G.; Bennett, M. A.; Tomkins, I. R. *J. Chem. Soc. Dalton Trans.* **1976**, 439.
(24) Grim, S. O.; Barth, R. C.; Mitchell, J. D.; Del Gaudio, J. *Inorg. Chem.* **1971**, *16*, 1776.
(25) Hietkamp, S.; Stuffken, D. J.; Vrieze, K. *J. Organometal. Chem.* **1979**, *169*, 107.
(26) Duffy, N. W.; McAdam, C. J.; Robinson, B. H.; Simpson, J. Paper in preparation.
(27) (a) Ranatunge-Bandarage P. R. R Thesis, University of Otago, 1989. (b) Duffy, N. W.; Robinson, B. H.; Simpson, J. Unpublished work.